JOURNAL OF MATERIALS SCIENCE 27 (1992) 4075–4079

Electrical characterization of semiconducting polycrystalline $Ga_xIn_{(1-x)}Sb$ alloys

P. P. SAHAY, M. SHAMSUDDIN*, R. S. SRIVASTAVA
*Department of Physics, and *Department of Metallurgical Engineering, Institute of Technology, Banaras Hindu University, Varanasi 221 005, India*

The electrical conductivity, Hall coefficient and mobility of the sintered pellets of semiconducting polycrystalline $Ga_xIn_{(1-x)}Sb$ alloys ($x = 0$, 0.1, 0.2, 0.3, 0.4, 0.5, 0.7, 0.8 and 1) have been determined in the temperature range 290–425 K. The variation of d.c. electrical conductivity with temperature has been explained by Seto's model. Samples with $x = 0.5$ and 0.7 have been found to show anomaly in Hall effect sign, while the sample with $x = 1$, i.e. GaSb, shows a Hall effect too small to be detected. Various kinds of scattering mechanisms under different temperature ranges have been observed in different alloy samples.

1. Introduction

The compound semiconductors GaSb and InSb, and the alloys based on them are of interest to semiconductor researchers [1–7] because of their wide application in electronic and optical devices, such as microwave rectifiers, tunnel diodes, Hall effect devices, infrared photocells, optical filters, etc. In recent years, polycrystalline semiconducting alloys have received special attention because their use in devices reduces the complications of ultrapurification and highly controlled conditions required for the growth of single crystals. In order to increase the reliability of devices it is of the utmost importance that electrical properties of such materials be fully investigated at different temperatures.

The aim of the present investigation was to attempt to prepare single-phase alloys of $Ga_xIn_{(1-x)}Sb$, and to study some of the properties, namely electrical conductivity, Hall coefficient and mobility, as a function of temperature and/or composition.

2. Experimental procedure

2.1. Materials

High-purity gallium and antimony (each 99.999% pure) and indium (99.99% pure) were used in this investigation.

2.2. Sample preparation

A series of alloys of $Ga_xIn_{(1-x)}Sb$ at different compositions ($x = 0$, 0.1, 0.2, 0.3, 0.4, 0.5, 0.7, 0.8 and 1) were prepared by pyrosynthesis of constituent elements. The specific elements in stoichiometric proportions, weighed to an accuracy of 10^{-5} g, were sealed in thick-walled transparent quartz capsules under a vacuum of $> 10^{-5}$ mm Hg. The capsules were heated at a rate of 3 K min^{-1} to 50 K above the liquidus temperature [8], and held for about 20 h with periodic shaking. The capsules were finally thoroughly shaken and allowed to cool to room temperature in the furnace.

The resultant mass was ground to fine powders ($-$ 100 μm) and compacted to pellets of 8 mm diameter and 1 mm thick. The pellets depending on composition were sintered at temperatures of about two-thirds their liquidus temperatures (in absolute scale) under a vacuum of $\sim 10^{-2}$ mm Hg. The thickness of the sintered pellets was measured using a micrometer screw gauge after polishing the pellets with 4/0 emery paper.

2.3. Sample characterization

2.3.1. *X-ray diffraction and scanning electron microscopic analyses*

X-ray diffraction profiles of all the sintered pellets were taken with a Philips PW 1710 diffractometer using CuK_{α_1} radiation to check the formation of single phase in the alloy samples. Pellets were also examined under a Jeol JSM-840A scanning electron microscope for morphological details.

2.3.2. *Electrical conductivity and Hall measurements*

D.c. electrical conductivity and Hall measurements were carried out using the standard Van der Pauw method [9, 10] in the temperature range 290–425 K. As shown in Fig. 1, the Van der Pauw four-probe assembly consisted of a four-wall enclosure made of asbestos sheet covered with glass tape to achieve constant temperature inside the enclosure. The enclosure was kept inside an insulating block fixed with heating elements. The top of the enclosure was covered with an insulating lid made of glass fibre sheet. Pressure contacts were made on the sample using spring-loaded probes fixed in the insulating lid. A

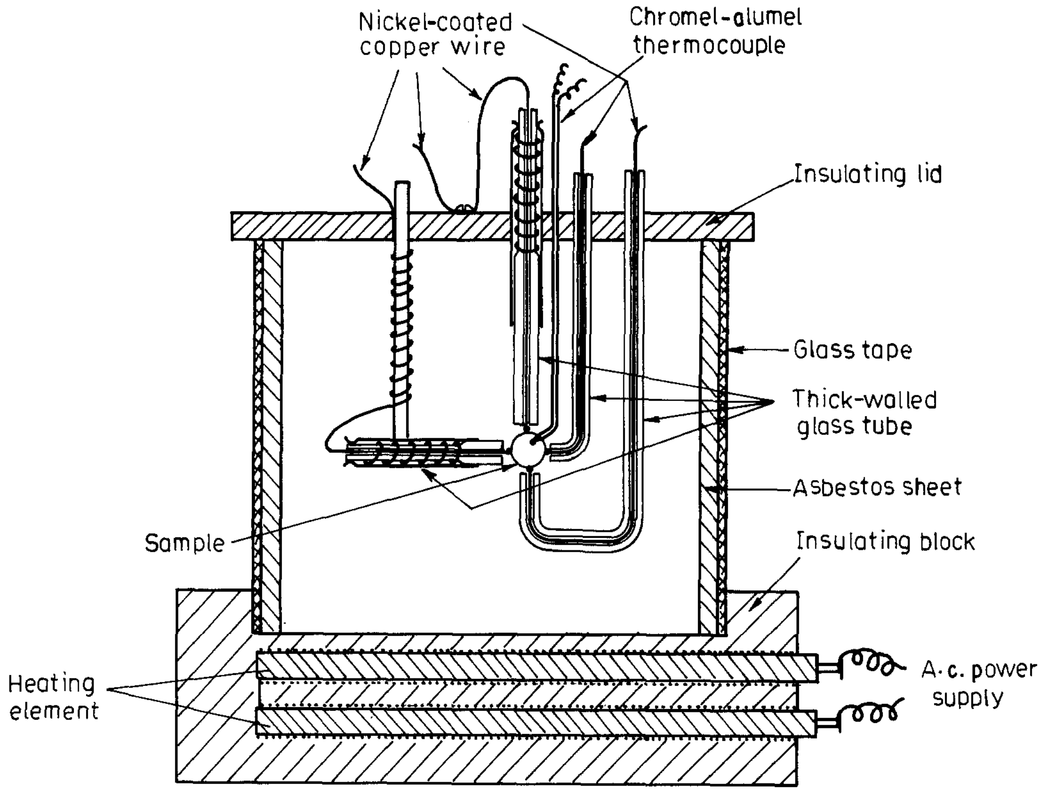

Figure 1 Schematic diagram of the Van der Pauw four-probe assembly.

Keithley 228 voltage/current source was used for constant current supply, and the voltage was measured using a Keithley 181 nanovoltmeter. The temperature of the assembly was controlled to an accuracy of $\pm 0.5\,^{\circ}\mathrm{C}$ by a PID digital temperature controller (Servotronics, India) and was monitored using a chromel–alumel thermocouple. For Hall measurements, an electromagnet (Polytronic, India) with magnetic field of about 9 kG was used.

2.3.3. Thermoelectric power measurements

Qualitative measurements of thermoelectric power at room temperature were conducted to determine the nature of current carriers in these samples.

3. Results and discussion

The results inferred from X-ray diffraction analysis of the sintered pellets of alloy samples indicate that GaSb and InSb are of single-phase intermetallic compounds while other alloys of $Ga_xIn_{(1-x)}Sb$ are closer to the two-phase region rather than the single phase. However, X-ray diffraction profiles obtained for alloys ($x = 0.1, 0.2, 0.3, 0.4, 0.5, 0.7$ and 0.8) are not characteristic of a material consisting of two completely separate phases. Instead of sharp lines, broad bands are obtained, the higher and lower angle edges of the band corresponding approximately to the positions of equivalent lines in the diffraction profiles for GaSb and InSb, respectively. Typical scanning electron micrographs of the sintered pellets of alloy samples with $x = 0, 0.2, 0.4, 0.5, 0.7$ and 1 are shown in Fig. 2a–f. From these micrographs it is clear that the samples have grains of different sizes. The presence of pores in the samples has also been observed in the micrographs.

The temperature dependence of electrical conductivity of all the samples is shown in Fig. 3. The nature of the current carriers in these samples determined by thermoelectric power measurements, has been indicated by "n" or "p" on each curve. The temperature coefficient of resistivity has been found to be negative throughout the temperature range investigated indicating that the samples are of semiconducting nature. At room temperature (291 K) the electrical conductivity as a function of composition is as shown in Fig. 4. It starts from a value of 43.47 $(\Omega\mathrm{cm})^{-1}$ for InSb, decreases to a minimum and then increases again to a value of 4.92 $(\Omega\mathrm{cm})^{-1}$ for GaSb. These values are much lower than the corresponding values for monocrystalline samples. This is expected because of the presence of grain boundaries in polycrystalline samples.

It has been observed that Group III–V elements have a tendency to form stoichiometric compounds even with slight departure from stoichiometric composition of the constituents [11]. The slight non-stoichiometric composition of the constituents, according to the segregation theory [12, 13], tends to segregate at the grain boundaries. These atoms at the grain boundaries have dangling bonds, resulting in a large number of trap centres in the forbidden gap of polycrystalline materials. These traps, depending on their concentration and energy level position with respect to the Fermi level, can trap the free charge carriers. These charged states at the grain boundaries create potential barriers which oppose the passage of carriers from one grain to the neighbouring ones. Above room temperature, the dominant transport

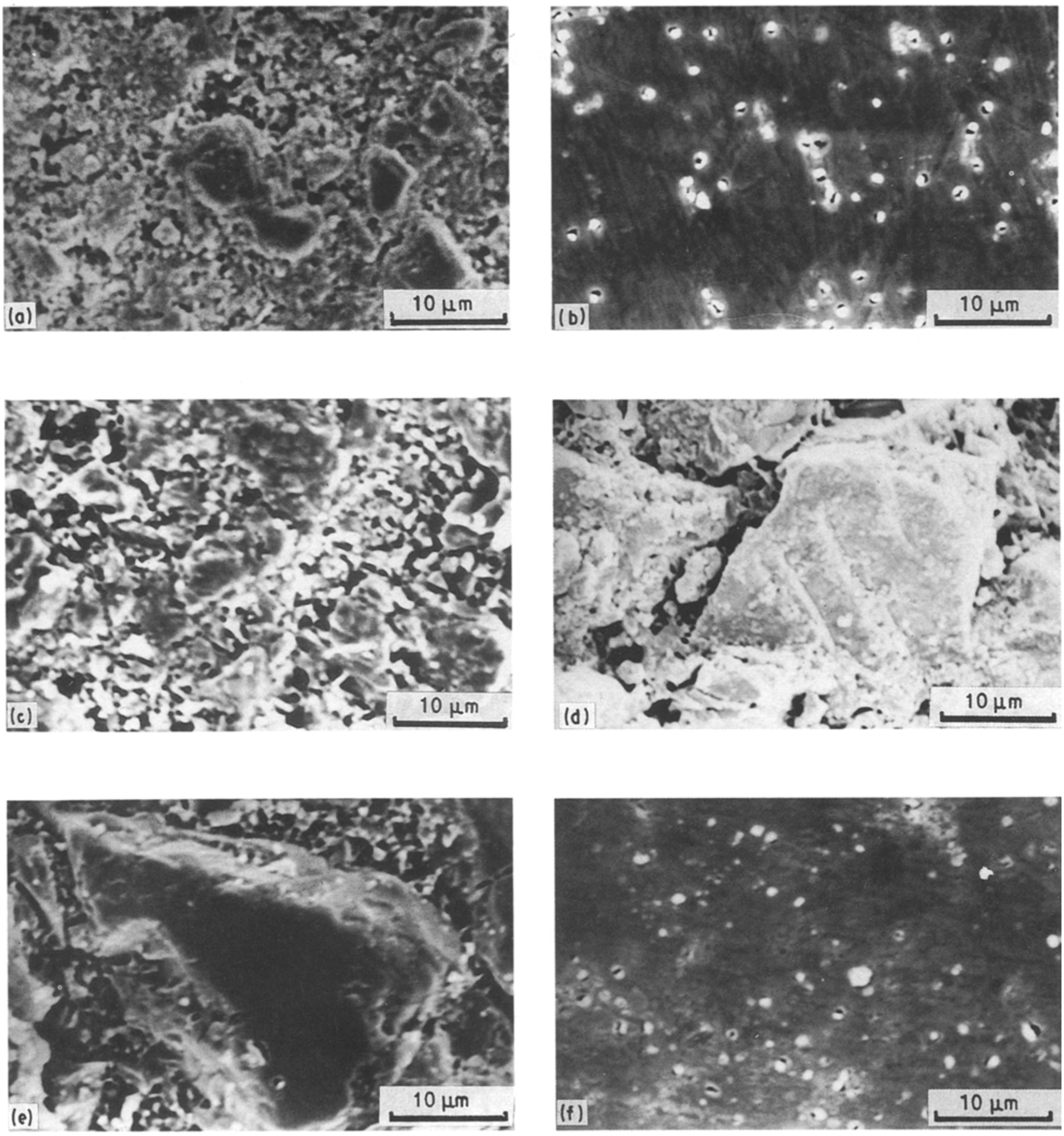

Figure 2 Scanning electron micrographs of sintered pellets of samples with $x = 0$; (b) 0.2; (c) 0.4; (d) 0.5; (e) 0.7; (f) 1.0.

mechanism in polycrystalline materials (e.g. polycrystalline silicon) is usually thermionic emission over the barriers. According to the grain-boundary trapping model proposed by Seto [14], when transport occurs by thermionic emission over the grain boundaries, the resistivity, ρ, is given by the expression

$$\rho = \frac{(2\pi m^* kT)^{1/2}}{q^2 L N_c} \exp(E_a/kT) \qquad (1)$$

where m^* is the effective mass of the charge carrier, L the average grain size of the sample, N_c the effective density of states in the conduction band of the sample, and E_a is the activation energy for the grain-boundary-limited conductivity. Other symbols have their usual meanings.

From the observed linearity of the plot of $\ln(\rho/T^{1/2})$ versus $1/T$, shown in Fig. 5, at all the compositions in the temperature range 290–350 K, it may be inferred that these results corroborate Seto's model. The departure from the linearity of the plot at higher temperatures in some samples ($x = 0.3$, 0.4, 0.7 and 1.0) has been attributed to a modification of the scattering process. Activation energies of conduction for all the samples have been estimated from the slope of $\ln(\rho/T^{1/2})$ versus $1/T$ plots. Variation of activation energy as a function of composition is shown in Fig. 6. It may be noted that alloys with larger activation energy for conduction have been found to possess high values of electrical conductivity compared to those with lower activation energy. This unusual feature can be well understood in terms of the involvement of

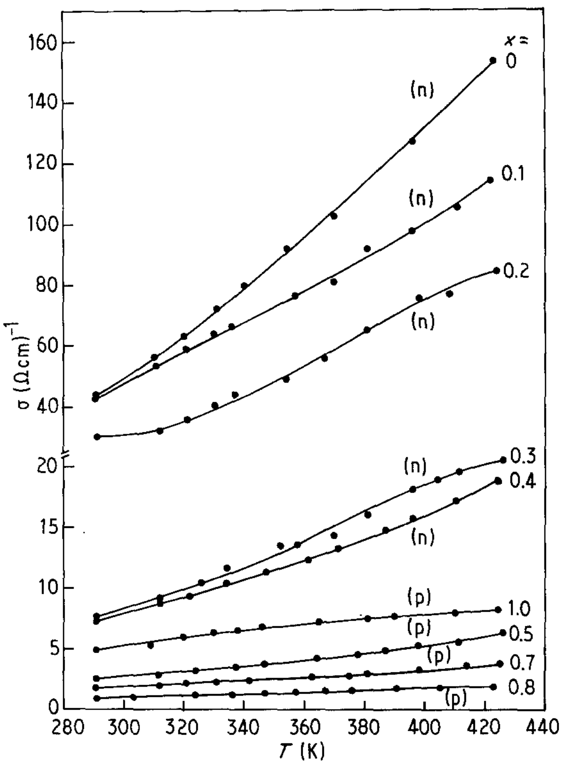

Figure 3 Electrical conductivity, σ, versus temperature plot of $Ga_xIn_{(1-x)}Sb$ alloys.

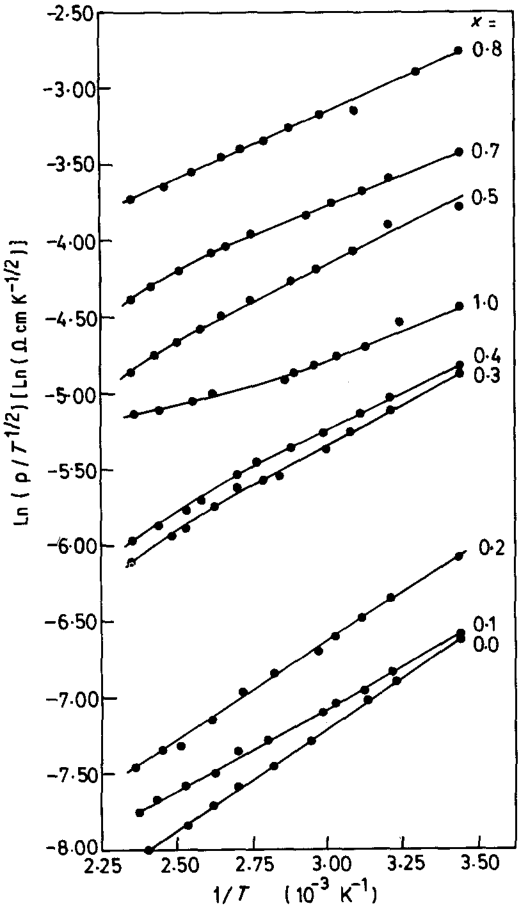

Figure 5 $\mathrm{Ln}(\rho/T^{1/2})$ versus $1/T$ plot of $Ga_xIn_{(1-x)}Sb$ alloys.

corresponding changes in the values of m^*, L and N_c in different alloys.

Fig. 7 shows the plot of $\ln|R_H|$ versus $1/T$. In the case of GaSb, the Hall effect is too small to be detected,

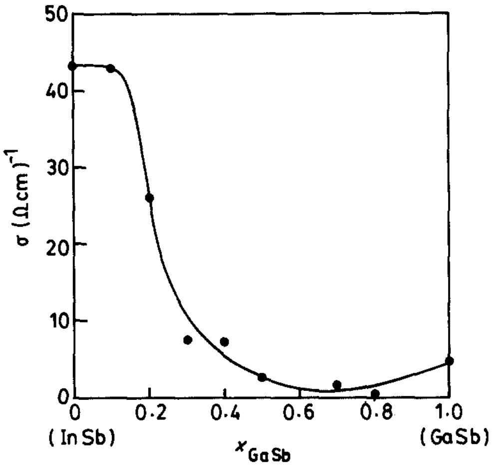

Figure 4 Electrical conductivity, σ, versus composition plot of $Ga_xIn_{(1-x)}Sb$ alloys at room temperature (291 K).

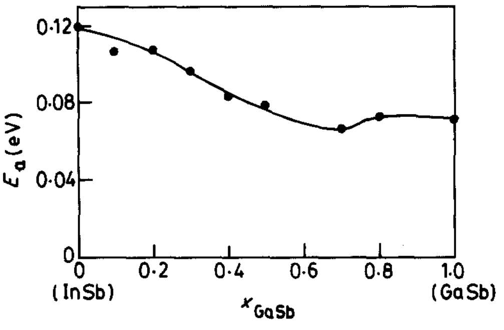

Figure 6 Activation energy, E_a, versus composition plot of $Ga_xIn_{(1-x)}Sb$ alloys.

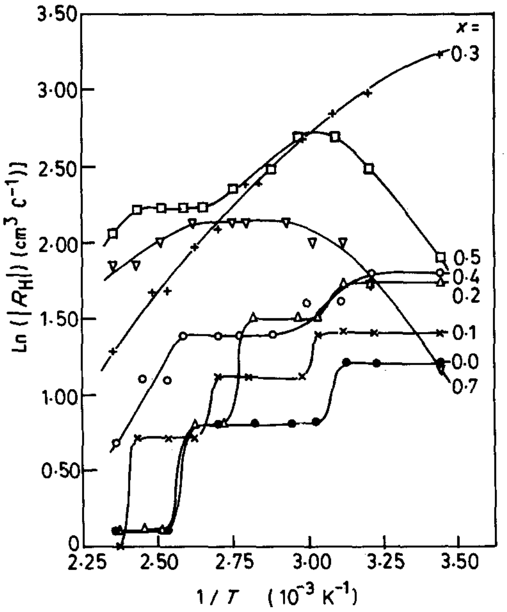

Figure 7 $\mathrm{Ln}|R_H|$ versus $1/T$ plot of $Ga_xIn_{(1-x)}Sb$ alloys.

which apparently may be due to the low mobility of charge carriers (holes). Samples with $x = 0.5$ and 0.7 show a Hall effect sign anomaly, i.e. p-type thermopower is associated with a negative Hall effect. This has been attributed to much lower mobility of holes relative to that of electrons in these materials [15]. Fig. 7 shows that samples with $x = 0$, 0.1, 0.2 and 0.4

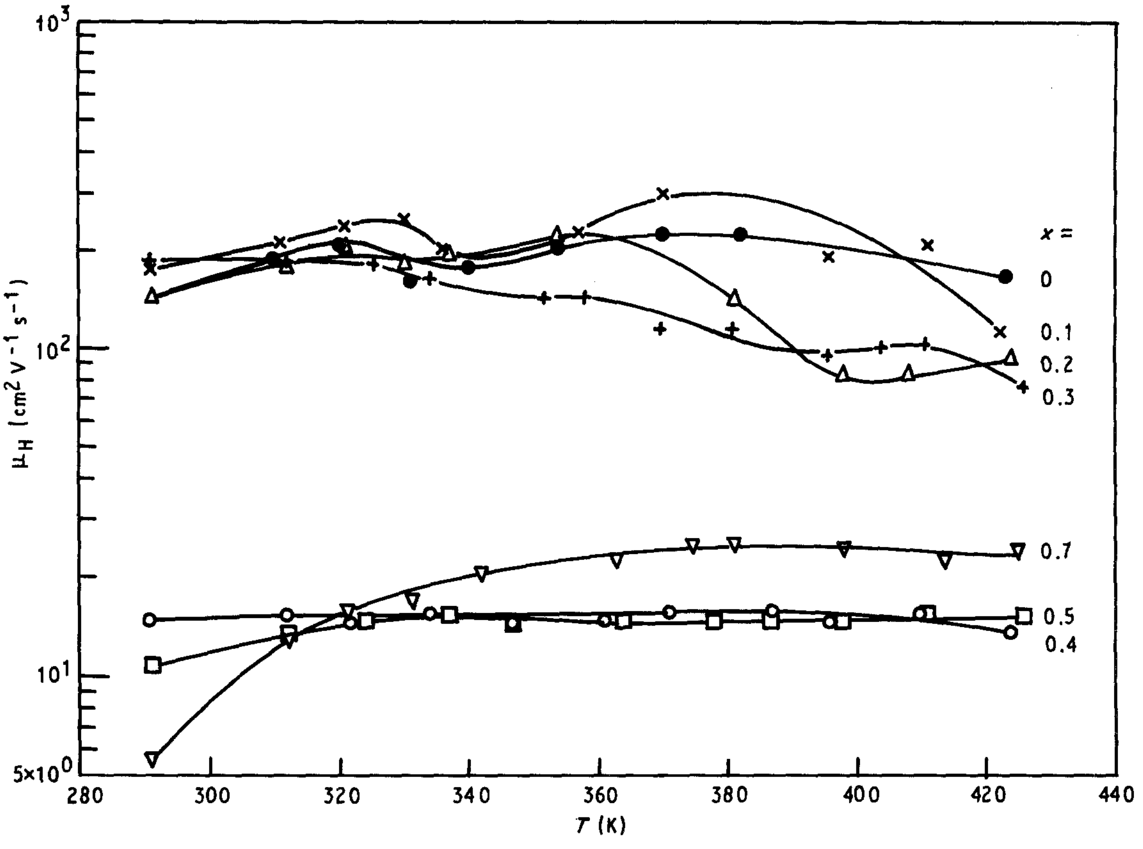

Figure 8 Hall mobility, μ_H, versus temperature plot of $Ga_xIn_{(1-x)}Sb$ alloys.

exhibit a similar type of variation in Hall coefficient with temperature. For the sample with $x = 0.3$, the Hall coefficient has been found to decrease exponentially with increasing temperature, while for samples with $x = 0.5$ and 0.7, it first increases sharply, reaches a maximum value and then decreases. These results can be explained in terms of the involvement of different kinds of scattering processes under different temperature ranges. This prediction is consistent with the observed variation of Hall mobility, μ_H, with temperature as shown in Fig. 8. It may be noted that observed increase of μ_H with temperature in the samples is due to the dominance of mobility limited by impurity scattering, while the observed decrease of μ_H with temperature has been attributed to the dominance of mobility limited by the scattering due to lattice vibrations.

Acknowledgements

The authors thank Professor V. B. Tare, Department of Metallurgical Engineering, Banaras Hindu University, Varanasi, for many valuable and useful discussions, and Mr S. N. Lal, Department of Metallurgical Engineering, Banaras Hindu University, Varanasi, for taking scanning electron micrographs of the samples. Financial assistance from the Ministry of Human Resources Development, Government of India, New Delhi is gratefully acknowledged.

References

1. W. F. SCHOTTKY and M. B. BEVER, *Acta Metall.* **6** (1958) 320.
2. C. D. KOURKOUTAS, G. I. PAPAIOANNOU, P. C. EUTHYMIOU and G. E. ZARDAS, *Solid State. Commun.* **67** (1988) 651.
3. M. ZEMPEL, M. OSZWALDOWSKI and J. GOC, *Acta Phys. Pol. A* (*Poland*) **A75** (1989) 297.
4. L. P. KRUKOVSKAYA, L. S. BERMAN, A. Y. VUL and A. Y. SHIK, *Sov. Phys. Semicond.* **11** (1977) 1109.
5. Y. NAGAO, T. HARIU and Y. SHIBATA, *IEEE Trans. Electron Devices* **ED-28** (1981) 407.
6. F. A. EGOROV and S. S. MURZIN, *Sov. Phys. JETP* **67** (1988) 1045.
7. M. L. KORWIN-POWCOWSKI and E. L. HEASEU, *Solid State Electron.* **18** (1975) 849.
8. L. M. FOSTER and J. F. WOODS, *J. Electrochem. Soc.* **118** (1971) 1175.
9. L. J. VAN DER PAUW, *Philips Res. Rept.* **13** (1958) 1.
10. *Idem, Philips Tech. Rev.* **29** (1959) 220.
11. C. HILSUM and A. C. ROSE-INNES, "Semiconducting III–V Compounds" (Pergamon, Oxford, 1961) p. 69.
12. M. E. COWER and T. O. SEDGWICK, *J. Electrochem. Soc.* **119** (1972) 1565.
13. A. L. FRIPP, *J. Appl. Phys.* **46** (1975) 1240.
14. J. Y. W. SETO, *ibid.* **46** (1975) 5247.
15. C. HILSUM and A. C. ROSE-INNES, "Semiconducting III–V Compounds" (Pergamon, Oxford, 1961) pp. 120–1.

Received 27 March
and accepted 23 July 1991